Design and Synthesis of Heterobimetallic Ru(II)−Ln(III) Complexes as Chemodosimetric Ensembles for the Detection of Biogenic Amine Odorants

ARTICLE *in* ANALYTICAL CHEMISTRY · JULY 2013

Impact Factor: 5.64 · DOI: 10.1021/ac401513j · Source: PubMed

3 AUTHORS, INCLUDING:

Cheuk-Fai Chow
The Hong Kong Institute of Education
42 PUBLICATIONS **689** CITATIONS
SEE PROFILE

Michael Lam
City University of Hong Kong
70 PUBLICATIONS **1,051** CITATIONS
SEE PROFILE

analytical chemistry

Article

pubs.acs.org/ac

Design and Synthesis of Heterobimetallic Ru(II)−Ln(III) Complexes as Chemodosimetric Ensembles for the Detection of Biogenic Amine Odorants

Cheuk-Fai Chow,*[,†,‡] Michael H. W. Lam,[§] and Wai-Yeung Wong[⊥]

[†]Department of Science and Environmental Studies, The Hong Kong Institute of Education, 10 Lo Ping Road, Tai Po Hong Kong SAR, China

[‡]Centre for Education in Environmental Sustainability, The Hong Kong Institute of Education, 10 Lo Ping Road, Tai Po Hong Kong SAR, China

[§]Department of Biology and Chemistry, City University of Hong Kong, 83 Tat Chee Ave., Hong Kong SAR, China

[⊥]Department of Chemistry, Hong Kong Baptist University, Waterloo Road, Kowloon Tong, Hong Kong SAR, China

Supporting Information

ABSTRACT: The detection of neutral biogenic amines plays a crucial role in food safety. Three new heterobimetallic Ru(II)−Ln(III) donor-acceptor complexes, KPrRu, KNdRu, and KSmRu, K{[$Ru^{(II)}$(^{t}Bubpy)$(CN)_4$]$_2$−$Ln^{(III)}(H_2O)_4$} (where ^{t}Bubpy = 4,4′-di-*tert*-butyl-2,2′-bipyridine), have been synthesized and characterized. Their photophysical and X-ray crystallographic data were reported in this study. These complexes were found to be selective for biogenic amine vapors, such as histamine, putrescine, and spermidine, with a detection limit down to the ppb level. The sensitivities of these complexes to the amines were recorded as ∼log K = 3.6−5.0. Submicron rods of the complexes, with a nanoscale diameter and microscale length, were obtained through a simple precipitation process. Free-standing polymeric films with different degrees of porosity were fabricated by blending the submicron rods with polystyrene polymer. The polymer with the highest level of porosity exhibited the strongest luminescence enhancement after amine exposure. Real time monitoring of gaseous biogenic amines was applied to real fish samples (Atlantic mackerel) by studying the spectrofluorimetric responses of the Ru(II)−Ln(III) blended polymer film.

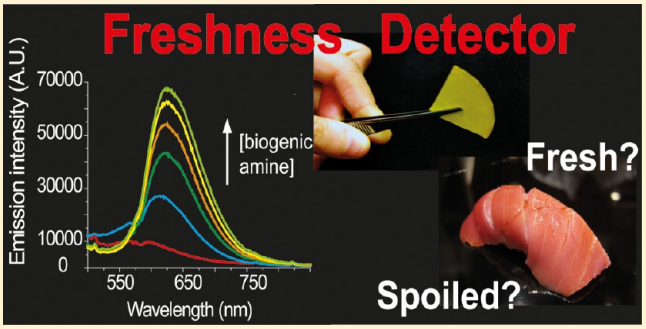

Volatile biogenic amines are well-known biomarkers of seafood freshness.[1−4] The link between the levels of biogenic amines with respect to the number of bacteria in fish and shrimp and other shelled species has been demonstrated.[2a−d] Histamine, which has been identified as a neurotransmitter,[2e,f] is the causative agent of scombroid poisoning, a foodborne chemical hazard.[2g−i] An intake of 8−40 ppm of histamine can lead to slight food poisoning, and an intake of more than 100 ppm can have serious effects on human health.[2g−i] According to the U.S. Food and Drug Administration, histamine levels should not exceed 50 ppm.[2j] This chemical can cause headaches, rashes, diarrhea, flushing, respiratory disorders, vomiting, and a life-threatening high blood pressure episode in sensitive individuals.[2k]

The qualitative and quantitative methods of analyzing biogenic amines recently described in the literature take advantage of chromatographic analytical methods such as gas chromatography, capillary electrophoresis, and high-performance liquid chromatography.[4] Molecular imprinting methods,[5a] enzymatic techniques,[5b−e] and immune assays[5f] are also used. However, what is vital is a method that allows the rapid and in situ detection of important biogenic amines and reporting of the signal in a naked-eyed manner. Supramolecular dosimeters or sensors based on a variety of compartments, such as organic dyes,[6] coordination complexes,[7] hydrogels,[8] polymers,[9] nanoparticles,[10] and arrays,[11] have been reported for amine detection.

Chemodosimeters are molecular devices that interact with analytes and yield physical signals in an irreversible fashion.[12] In contrast to chemosensors, which counter their analyte in real-time fashion, chemodosimeters react with their analyte in a cumulative manner.[13] This property renders chemodosimeters particularly suitable for food quality monitoring. Because the chemodosimetric signal indicating spoilage cannot be reversed, it leaves operators/customers in no doubt that contamination has occurred.

Research attention has recently focused on the development of new molecular detection systems for the in situ monitoring

Received: May 15, 2013
Accepted: July 25, 2013
Published: July 25, 2013

   dx.doi.org/10.1021/ac401513j | *Anal. Chem.* 2013, 85, 8246−8253

Scheme 1. Design Concept of Heterobimetallic Ensembles, Ru(II)−Ln(III) for the Detection of Biogenic Amines (Histamines, Putrescine, Spermidine, and Ammonia)

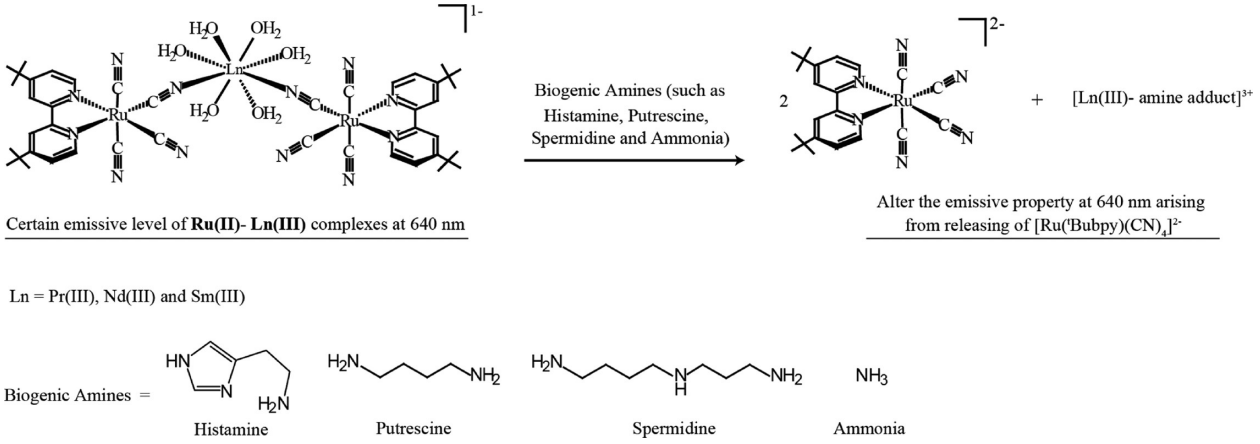

of analytes.[14] Indicator displacement assay,[15−17] a new molecular detection approach, has been applied to determine anions,[15a,b,16a,b,17c,d] neutral organic molecules,[15e] zwitterions,[15c,d,16c,d,17a,b] and other molecules.[15e] This assay involves the initial binding of an indicator to a receptor, thereby forming an "ensemble." A targeted analyte is introduced into the system, causing the displacement of the indicator from the receptor, which in turn supplies an optical signal. The approach has the advantages of good analyte selectivity, high sensitivity, and rapid and reliable assays. Ensembles usually comprise two organic counterparts or one organic plus one metal counterpart.[15−17] The research groups led by Anslyn,[15] Fabbrizzi,[16] and Martınez-Manez[17] are the pioneers of this type of assay. Our group is focusing on the feasibility of using M_A−C≡N−M_B bimetallic complexes as chemodosimeters (M_A = Fe^{II}, Ru^{II}, and Os^{II}; M_B = Pt^{II}, Cu^{II}, Ni^{II}, and Eu^{III}) for the detection of various analytes.[7a,18] We envision that, with suitable metal ions combinations, heterobimetallic chemodosimeters with fine-tuned analyte specificity can be obtained.

The immobilization or encapsulation of a molecular sensor or dosimeter into a solid-state material constitutes an important step for applicable systems.[19] However, a fundamental challenge is detection of a gaseous analyte by a solid active material in a sensitive and fast manner. Studies using bimetallic complexes as solid-stated sensing or dosimetric materials remain sparse.[20] This paper reports the synthesis and characterization of three new Ru(II)−Ln(III) ensembles: K{[$Pr(H_2O)_4$]−[Ru(^{t}Bubpy)$(CN)_4$]$_2$} (KPrRu), K{[$Nd(H_2O)_4$]−[Ru(^{t}Bubpy)$(CN)_4$]$_2$} (KNdRu), and K{[$Sm(H_2O)_4$]−[Ru(^{t}Bubpy)$(CN)_4$]$_2$} (KSmRu) (^{t}Bubpy = 4,4′-di-*tert*-butyl-2,2′-bipyridine). A conceptual scheme for a competitive displacement assay for biogenic amines using these heterobimetallic ensembles is shown in Scheme 1. The ensembles were found to produce specific naked-eyed luminescent responses to biogenic amines down to 10 ppb. The rod-like morphologies of KPrRu, KNdRu, and KSmRu can be obtained at the submicrometer scale through a simple precipating process. Further, no surfactant is needed to assist in the fabrication of these submicrometer structures.

EXPERIMENTAL SECTION[21]

K{[$Pr(H_2O)_4$]−[Ru(^{t}Bubpy)$(CN)_4$]$_2$}·8H_2O (KPrRu). A mixture of K_2[Ru(^{t}Bubpy)$(CN)_4$] (0.110 g, 0.2 mmol) and $Pr(CH_3COO)_3$·hydrate (0.032 g, 0.1 mmol) was stirred in 5 mL of a water/methanol mixture (1:1) at room temperature for 30 min and then allowed to stand overnight. Yellow crystalline plates were obtained through the slow evaporation of the solvent. Yield: 0.0.091 g (69%). IR (KBr): $\nu_{C\equiv N}$ = 2063, 2101 cm^{-1}. ESI-MS (-ve mode): *m*/*z* 1089 {[Pr]−[Ru(^{t}Bubpy)$(CN)_4$]$_2$}$^-$. Anal. Calcd. for $C_{44}H_{56}KN_{12}O_4PrRu_2$·7$H_2O$: C, 39.88; H, 5.32; N, 12.68. Found: C, 40.16; H, 5.35; N, 12.99.

K{[$Nd(H_2O)_4$]−[Ru(^{t}Bubpy)$(CN)_4$]$_2$}·8H_2O (KNdRu). The synthetic procedure was similar to that for complex KPrRu except that $Nd(NO_3)_3$·hydrate (0.033 g, 0.1 mmol) was used instead of $Pr(CH_3COO)_3$·hydrate. Yellow crystalline plates were again obtained through the slow evaporation of the solvent. Yield: 0.0.101 g (75%). IR (KBr): $\nu_{C\equiv N}$ = 2063, 2102 cm^{-1}. ESI-MS (-ve mode): *m*/*z* 1091 {[Nd]−[Ru(^{t}Bubpy)$(CN)_4$]$_2$}$^-$. Anal. Calcd. for $C_{44}H_{56}KN_{12}NdO_4Ru_2$·8$H_2O$: C, 39.25; H, 5.39; N, 12.48. Found: C, 39.04; H, 5.36; N, 12.71.

K{[$Sm(H_2O)_4$]−[Ru(^{t}Bubpy)$(CN)_4$]$_2$}·8H_2O (KSmRu). The synthetic procedure was similar to that for complex KPrRu except that $Sm(NO_3)_3$·6H_2O (0.046 g, 0.1 mmol) was used instead of $Pr(CH_3COO)_3$·hydrate. Yellow crystalline plates were obtained through the slow evaporation of the solvent. Yield: 0.0.087 g (65%). IR (KBr): $\nu_{C\equiv N}$ = 2065, 2103 cm^{-1}. ESI-MS (-ve mode): *m*/*z* 1099 {[Sm]−[Ru(^{t}Bubpy)$(CN)_4$]$_2$}$^-$. Anal. Calcd. for $C_{44}H_{56}KN_{12}O_4Ru_2Sm$·7$H_2O$: C, 39.59; H, 5.29; N, 12.59. Found: C, 40.55; H, 5.41; N, 12.88.

UV−Vis Spectroscopic and Spectrofluorimetric Titrations. All solvents used in the UV−vis spectroscopic and spectrofluorimetric titrations were of analytical grade, and all of the titrations were carried in ethanol. Measurements were taken after equilibrium had been reached between the receptor and substrate. A 1:2 receptor−substrate interaction was analyzed according to the Benesi−Hildebrand equations for spectrofluorimetric titration.[21]

Submicrometer Material Preparation. KPrRu, KNdRu, and KSmRu were dissolved in 1.0 mL of ethanol with concentrations of 2 × 10^{-3} M. Ether (2000 μL) was added to the ethanolic solutions (50 μL) to produce a fine suspension in each case. The suspension (1000 μL) was pipetted into an Eppendorf tube and evaporated at room temperature, and 1.5 mL of distilled water was then added to the Eppendorf tube. The aqueous solution was ultrasonic for 15 min. The solution was dropped onto a silicon wafer for air-drying. The morphologies of the submicrometer structures that had been formed were examined by scanning electron microscopy

dx.doi.org/10.1021/ac401513j | *Anal. Chem.* 2013, 85, 8246−8253

(SEM). A beam energy of 80 keV was used, and the bright field high-resolution mode was selected. The magnification varied from around 5000× to 100k×. Energy-dispersive X-ray spectrometry (EDS) analyses were also performed to determine the composition of the sample.

RESULTS AND DISCUSSION

Synthesis and Characterization. KPrRu, KNdRu, and KSmRu were formed by stirring two equivalents of $K_2[Ru(^tBubpy)(CN)_4]$ complex[22] with one equivalent of $Nd(NO_3)_3$·hydrate, $Sm(NO_3)_3·6H_2O$, and $Pr(CH_3COO)_3$·hydrate, respectively, in a 1:1 volume ratio of water/methanol mixture in open atmosphere at room temperature. All of the heterobimetallic complexes were isolated as air-stable yellow crystalline plates with a reasonable yield, and they were characterized by X-ray crystallography, electrospray ionization mass spectrometry (ESI-MS), infrared (IR) spectroscopy and microanalysis.

KPrRu, KNdRu, and KSmRu are isostructural. All of the crystal structures of the complexes are one-dimensional polymer chains with corresponding $K[Ln^{III}(H_2O)_4]-[Ru^{II}(^tBubpy)(CN)_4]_2$ repeating units. Figure 1 shows the perspective views of the crystal structures of KPrRu, KNdRu, and KSmRu. A one-dimensional linear polymer chain is formed along the *b*-axis of KLnRu (Figure 1a–c). The Pr(III), Nd(III), and Sm(III) ions in the titled complexes have 8-coordinated geometry which can be viewed as a distorted square antiprism with two basal planes made by atoms N3, N4, N5, and N6 and O1, O2, O3, and O4. For a regular square antiprism, two square planes are parallel to each other. However, in all of the mentioned lanthanide geometries, the two planes are unparallel with dihedral angles ~4.0°. The monomeric units of KLnRu are shown at the Supporting Information (S. Figure 1a–c), where two crystallographically independent $[Ru^{II}(^tBubpy)(CN)_4]^{2-}$ units and one Ln(III) center form a V-shaped configuration connected with two Ru–C≡N–Ln cyanide bridges. In each independent $[Ru^{II}(^tBubpy)(CN)_4]^{2-}$ unit, two axial cyanides are the bridging ligands and two equatorial cyanides are the nonbridging ligands. For the three complexes, the average bond distances between the Ln(III) centers [Pr(III), Nd(III), and Sm(III)] and cyano-N are calculated as 2.535 (13), 2.523 (15), and 2.488 (17) Å, respectively. Faulkner and Ward[20a–e] have described similar molecular configurations in two analogous complexes, that is, two-dimensional sheet neutral $\{[Ru(bpy)(CN)_4]_3-[Ln(H_2O)_4]_2\}$ complexes (where Ln = Nd and Gd) and discrete bent shape molecular $K\{[Ru(bpy)(CN)_4]_2[Ln(H_2O)_m]\}$ complexes (where Ln = Pr, Er, Yb; *m* = 7, 6, 6). The average bond distances of KPrRu, KNdRu, and KSmRu are summarized in Table 1, and the crystallographic data of the complexes are summarized in Supporting Information (S. Table 1). Details of the bond angle and length are summarized in Supporting Information (S. Tables 2–4).

Formation of the cyano-bridged bimetallic complex was also confirmed by IR spectroscopic studies in which the $\nu_{C\equiv N}$ of $K_2[Ru(^tBubpy)(CN)_4]$ at 2042, 2057, 2073, and 2096 cm^{-1} was altered to two new $\nu_{C\equiv N}$ bands, one in a range of approximately 2063 cm^{-1} and the other just above 2010 cm^{-1}, after coordinating to Ln(III). Characterizations of the solvated forms of KPrRu, KNdRu, and KSmRu were performed in organic solvent. All three complexes are soluble in polar organic solvents such as ethanol, methanol, dimethylsulfoxide (DMSO), and *N*,*N*-dimethylformamide (DMF). When dissolved in polar solvents, the complexes readily dissociate into their solvated monomeric units. The integrity of the cyanide bridges of the monomeric units of complexes KPrRu, KNdRu, and KSmRu in ethanol is demonstrated by their electrospray mass spectra showing peaks at *m*/*z* 1089 $\{[Pr]-[Ru(^tBubpy)(CN)_4]_2\}^-$, *m*/*z* 1091 $\{[Nd]-[Ru(^tBubpy)(CN)_4]_2\}^-$, and *m*/*z* 1097 $\{[Sm]-[Ru(^tBubpy)(CN)_4]_2\}^-$.

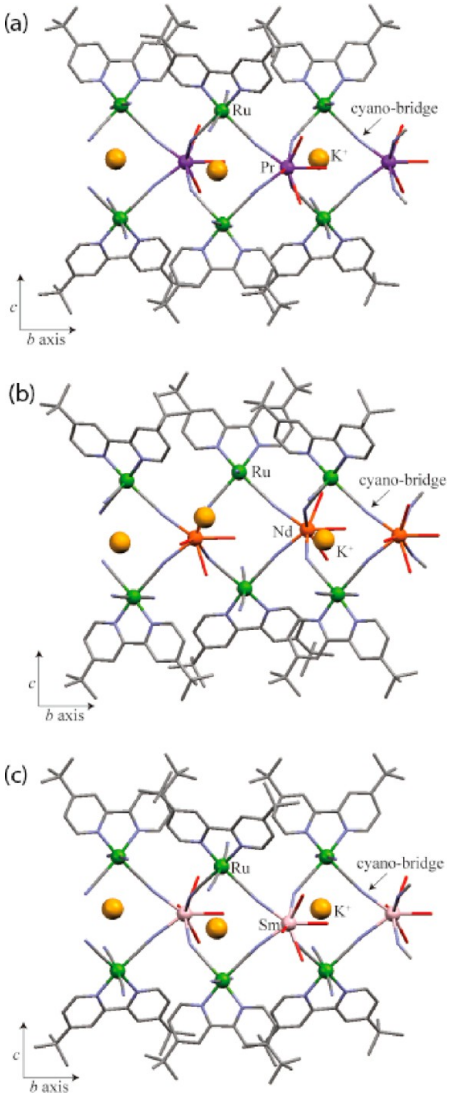

Figure 1. Perspective views of part of the one-dimensional chain structure in (a) KPrRu; (b) KNdRu; and (c) KSmRu along the *b* axis. Hydrogen atoms and noncoordinated water molecules were omitted for clarity (Pr in purple; Nd in orange; Sm in pink; Ru in green; C in gray; O in red; N in blue; K in yellow).

Table 1. Selected Mean Interatomic Distances (Å) from the Structures of Complexes KPrRu, KNdRu, and KSmRu

	KPrRu	KNdRu	KSmRu
Ru–CN (nonbridged)	2.035 (24)	2.043 (5)	2.040 (8)
Ru–CN (bridged)	1.958 (13)	1.975 (13)	1.970 (14)
C≡N (nonbridged)	1.163 (28)	1.148 (5)	1.150 (14)
C≡N (bridged)	1.168 (10)	1.158 (10)	1.168 (10)
Ln–N	2.535 (13)	2.523 (15)	2.488 (17)
K–C	3.283 (76)	3.275 (78)	3.270 (71)
K–N	3.318 (94)	3.310 (93)	3.312 (76)

Electronic Absorption and Luminescent Properties. The photophysical properties of the $K_2[Ru(^tBubpy)(CN)_4]$

dx.doi.org/10.1021/ac401513j | Anal. Chem. 2013, 85, 8246–8253

donor unit are known to be strongly dependent on its environment.[23] Previous spectroscopic work shows that the interaction between the lone-pair electrons of the cyanide ligands and surrounding electron-accepting ions/molecules affects the energy of the Ru(dπ) → ^{t}Bubpy (π^*) MLCT absorption band and ^{3}MLCT emissions.[24] The MLCT absorption among $K_2[Ru(^{t}Bubpy)(CN)_4]$, KPrRu, KNdRu, and KSmRu is summarized in Supporting Information (S. Figure 2a). The ethanolic solution of $K_2[Ru(^{t}Bubpy)(CN)_4]$ is yellow in color, with UV−vis absorption λ_{max} at 435 nm. Upon coordination to become KPrRu, KNdRu, and KSmRu, the MLCT absorption band of the Ru(II)−diimine chromophore blue-shifts from 435 to ∼417 nm.

The ^{3}MLCT emissions of the complexes are summarized in Supporting Information (S. Figure 2b). The ethanolic solution of $K_2[Ru(^{t}Bubpy)(CN)_4]$ produces strong luminescence at λ_{max} 654 nm with a lifetime of 97 ns. The ^{3}MLCT emissions of KPrRu and KSmRu are blue-shifted to ∼612 nm and are more intense and have longer lifetimes of 200 and 190 ns, respectively. On the other hand, the ^{3}MLCT emission of KNdRu is blue-shifted to 640 nm with a drastic diminishment in luminescent intensity and has a shorter lifetime at 90 ns.The concomitant blue shift in both the MLCT electronic transition and ^{3}MLCT emission in KLnRu is understandable in terms of the electron-withdrawing effect of the Ln(III) acceptor on stabilizing the *d*-orbitals of the Ru(II)−diimine chromophore. This effect is consistent with those observed in a number of related solvatochromic systems in which protons,[23] boron halides,[25] and transition-metal ions[26] act as Lewis acids.

Binding Properties of KPrRu, KNdRu, and KSmRu with Various Vapors. Figure 2a,b shows the UV−vis spectroscopic and spectrofluorometric titrations of KPrRu with histamine. Upon the addition of histamine to KPrRu, the MLCT transitions of the complex shift from 417 to 438 nm (Figure 2a), and the ^{3}MLCT emissions move from 644 to 656 nm with a significant decline in intensity (Figure 2b). By plotting the best fitted graph, $I_0/(I - I_0)$ versus $1/[\text{histamine}]^2$, the slope and *y*-intercept were calculated as −3.387 and -3.569×10^{-8} M^2, respectively (Figure 2c). The formation constant (log *K*) of KPrRu toward histamine was determined as 3.99 ± 0.04 by fitting the titration curves with the Benesi−Hildebrand equation [Supporting Information: eq (i)].[21,27] This equation suggests that each Pr(III) center in KPrRu binds two molecules of histamine. Figure 2d summarizes the spectrofluorimetric titrations of KPrRu (2.0×10^{-4} M) with common vapors, including biogenic amines (histamine, putrescine, spermidine, and ammonia) and other gases (aniline, H_2S, CO, CH_4, H_2, N_2, and atmospheric air). Only those vapors/gases with aliphatic amino functionality (histamine, putrescine, spermidine, and NH_3) are able to induce a spectrofluorometric response. Aromatic amino functionality, such as that featured by aniline and other common moieties, are unable to induce any observable spectrofluorometric changes. Thus, KPrRu is envisioned to respond solely to aliphatic amino-containing molecules. The spectrofluorimetric titrations (the mole ratio plot) of KPrRu to the biogenic amines reveal that the maximum response occurs at KPrRu versus analytes in a mole ratio of 1:2, which further confirms the 1:2 stoichiometry. Figure 2e presents a photograph of the naked-eye luminometric responses of KPrRu to various amine vapors and gaseous analytes. The vapors of histamine, putrescine, spermidine, NH_3, aniline, H_2S, CO, CH_4, H_2, N_2, and atmospheric air were purged into the headspace of the ethanolic solutions of KPrRu

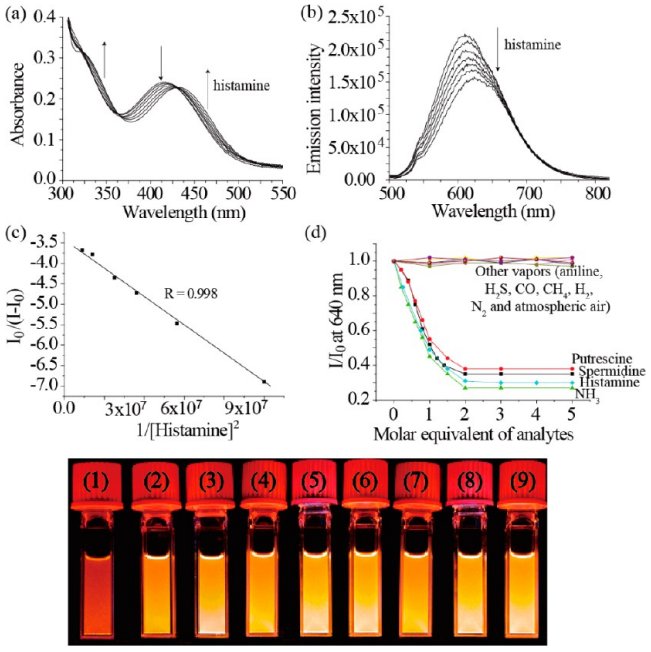

Figure 2. (a) UV−vis spectroscopic and (b) spectrofluorimetric titrations of KPrRu (3.33×10^{-5} M) with histamine (0 to 6.67×10^{-4} M). (c) The best fitted $I_0/(I - I_0)$ versus $1/[\text{histamine}]^2$ plot with log $K = 3.99 \pm 0.04$ at 640 nm (the slope and *y*-intercept are −3.387 and -3.569×10^{-8} M^2, respectively). (d) Summary of spectrofluorometric titration (I/I_0 at 640 nm) of KPrRu (2.0×10^{-4} M) to various analytes monitored as a function of increasing their concentration. All titrations were carried out in EtOH at 298 K with excitation at 466 nm. (e) Photos of the luminometric responses of the KPrRu (1.0×10^{-4} M) in EtOH at 298 K. (1) KPrRu + histamine; (2) KPrRu only; (3) KPrRu + aniline; (4–9) KPrRu + H_2S, CO, N_2, CH_4, H_2, and air respectively. Excitation λ_{ex} = 365 nm.

(2.0×10^{-4} M) at 298 K. The purging volume was 3 cm^3 for all of these analytes. Of the gases, only those with aliphatic amino functionality were able to induce naked-eye responses (Supporting Information S. Figures 3−6).

The UV−vis spectroscopic titrations of KNdRu with histamine are shown in the Supporting Information S. Figure 7a. Similar to KPrRu, upon the addition of histamine to the ethanolic solutions of KNdRu, the MLCT transitions of the complex shift from 417 to 438 nm. The spectrofluorometric titrations of KNdRu with histamine are shown in the Supporting Information S. Figure 7b. In this case, significantly different from those of KPrRu, the ^{3}MLCT emissions of KNdRu shift from 644 to 656 nm with a significant enhancement in intensity. The slope and *y*-intercept were calculated as 3.650 and 1.341×10^{-9} M^2, respectively, by plotting the best fitted $I_0/(I - I_0)$ versus $1/[\text{histamine}]^2$ graph (Supporting Information S. Figure 7c). The log *K* of KNdRu toward histamine was determined as 4.72 ± 0.01 by fitting the curves with the equation [Supporting Information: eq (i)].[21,27] The spectrofluorimetric titrations of KNdRu (2.0×10^{-4} M) with the common vapors and a photograph of the naked-eyed luminometric responses of KNdRu to various gaseous analytes are summarized in the Supporting Information (S. Figure 7d,e, respectively). S. Figures 8−11, Supporting Information, summarize the binding properties of the gases (histamine, putrescine, spermidine, and NH_3) with aliphatic amino functionality to KNdRu.

dx.doi.org/10.1021/ac401513j | *Anal. Chem.* 2013, 85, 8246−8253

The UV−vis spectroscopic and spectrofluorometric titrations of KSmRu with histamine are shown in Supporting Information (S. Figure 12a,b, respectively). The results are similar to those for KPrRu. The addition of histamine to the ethanolic solutions of KSmRu causes the MLCT transitions of the complex to shift from 417 to 437 nm and the ^{3}MLCT emissions to move from 610 to 640 nm, with a significant decline in intensity. The slope, y-intercept, and log K were calculated as −6.109, -6.320×10^{-9} M^2, and 4.72 ± 0.01, respectively, by plotting the best fitted $I_0/(I - I_0)$ versus 1/[histamine]^2 (Supporting Information S. Figure 12c). The spectrofluorimetric titrations and naked-eye luminometric responses of KSmRu (2.0×10^{-4} M) with the common vapors are summarized in the Supporting Information (S. Figure 12d,e, respectively, as well as S. Figures 13−16). Table 2 summarizes log K and detection limits of KPrRu, KNdRu, and KSmRu with the analytes in EtOH at 298 K.

Table 2. Log K and Detection Limits (in the Brackets) of KPrRu, KNdRu, and KSmRu with Histamine, Putrescine, Spermidine, Aniline, NH_3, H_2S, CO, CH_4, H_2, N_2, and Atmospheric Air in EtOH at 298 K

	KPrRu	KNdRu	KSmRu
histamine	4.00 (90 ppb)	4.72 (15 ppb)	4.52 (30 ppb)
putrescine	4.03 (60 ppb)	4.99 (10 ppb)	4.71 (50 ppb)
spermidine	4.02 (80 ppb)	4.80 (10 ppb)	4.14 (50 ppb)
NH_3	3.57 (250 ppb)	4.05 (110 ppb)	3.72 (180 ppb)
aniline	0.91 (80 ppm)	0.83 (30 ppm)	0.73 (70 ppm)
other vapors	–[a]	–[a]	–[a]

[a]Log K and detection limits were too small to be detected and calculated.

The close resemblance of the luminescence responses (both lifetime and excitation spectroscopic properties) of the KPrRu−histamine, KNdRu−histamine, and KSmRu−histamine mixtures to those of $K_2[Ru(^tBubpy)(CN)_4]$ suggests that the cyanide bridges between Ru$^{(II)}$ and the lanthanide ions of the trinuclear complex are cleaved after histamine binding to the lanthanide centers. The subsequent observation of $\{K[Ru(^tBubpy)(CN)_4]\}^-$ (m/z 513 $[M + K]^-$) in the ESI-MS of the KPrRu/KNdRu/KSmRu−histamine mixtures further confirmed this suggestion. The substrate selectivity of the binding-induced dissociation may be attributable to the preferential coordination of amino functionalities to the metallic lanthanide center. Scheme 1 shows the proposed recognition and signaling mechanism of the heterobimetallic complexes toward biogenic amines.

Submicrometer KLnRu Materials. To develop solid-supported dosimetric materials that can detect volatile analytes in a sensitive and fast process, the morphology (size, shape, and surface area) of the active materials and porosity of the solid-supported polymer were investigated. Here, we describe a control process for the precipitation of KLnRu and their formation of submicrometer scale materials. The morphologies of the submicrometer structures of KLnRu that were formed by the precipitating ethanolic solutions (50 μL, 2×10^3 M) into Et_2O (2 mL) were examined via SEM. The samples for these experiments were prepared by drop-casting the suspensions onto a silicon wafer substrate.

Figure 3a presents the SEM images of the dispersed KPrRu submicrorods with a diameter of 105 ± 10 nm and length, in micrometers, of 1.4 ± 0.6 μm. The chemical composition of these submicrostructures was determined by EDS (Figure 3a right). The peaks of Ru, Pr, K, C, and O were found (the Cu and Mo peaks originated from the Cu/Mo substrate), indicating that the crystals are products of KPrRu. Figure 3b shows the SEM images of the dispersed KNdRu submicrorods with a diameter of 230 ± 15 nm and length in the micrometer span (12.1 ± 0.6 μm). The chemical composition of an individual wire was determined by EDS (Figure 3b right). The peaks of Ru, Nd, K, C, and O were found, indicating that the structures are products of KNdRu. The SEM images (Figure 3c) revealed that the dispersion of KSmRu contains similar submicrorods with a diameter of 150 ± 50 nm and micrometer length span (1.0 ± 0.2 μm). EDS (Figure 3c right) revealed the peaks of Ru, Sm, K, C, and O, indicating that the colloids are products of KSmRu. Table 3 summarizes the shapes and sizes of the precipitation structures of KPrRu, KNdRu, and KSmRu.

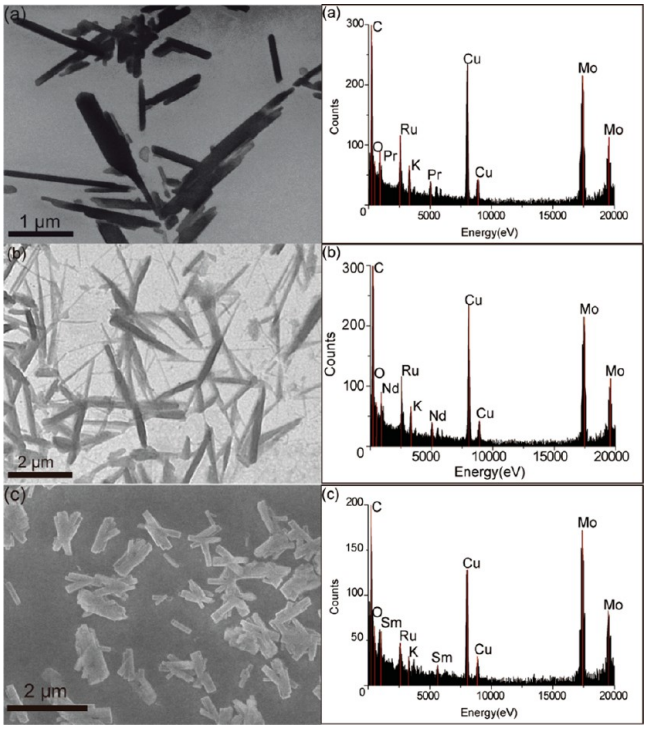

Figure 3. SEM images and EDS of (a) KPrRu; (b) KNdRu; and (c) KSmRu.

Table 3. Shape and Size of the Precipitation Structures of KPrRu, KNdRu, and KSmRu

	KPrRu	KNdRu	KSmRu
shape	rod	rod	rod
length/diameter (μm)	1.4 ± 0.6	2.1 ± 0.6	1.0 ± 0.2
width (nm)	105 ± 10	230 ± 15	150 ± 50

A high degree of stability and permanent porosity are among the other requirements for the general applicability of solid-supported chemodosimetric materials.[28] Regular pores, with sizes from the microscale, patterned into various kinds of solid-supported materials have been achieved through sophisticated techniques.[29] Solid-supported chemodosimetric materials were fabricated by blending the KNdRu submicrorods with polystyrene polymer. Three yellow free-standing films were obtained after evaporation of the suspension in dichloromethane at room temperature with an air flow rate of 0, 12, and

dx.doi.org/10.1021/ac401513j | Anal. Chem. 2013, 85, 8246−8253

24 L/min [Figure 4a–c right)]. Figure 4c (left) presents the SEM images of the surface of the polystyrene polymer film

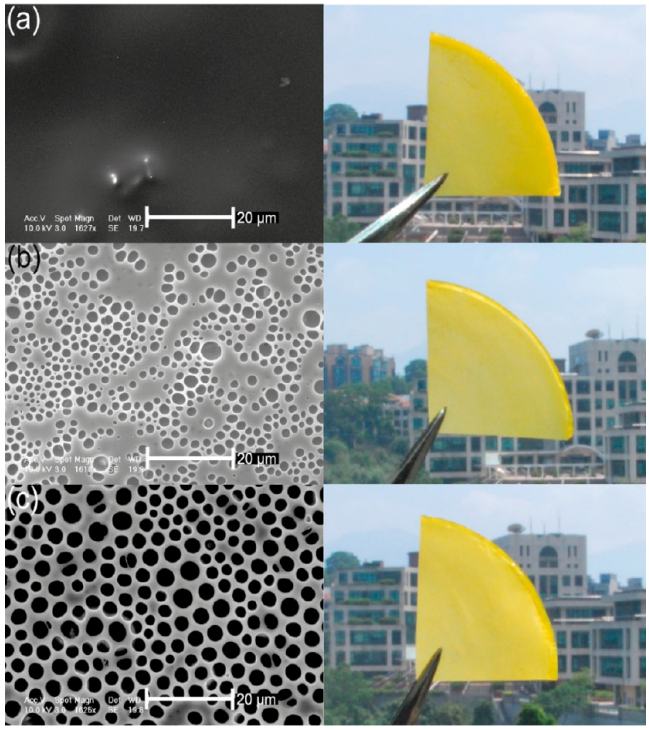

Figure 4. (Left) SEM images of the surface of polystyrene polymer film where KNdRu were immobilized. The porosity on the film was controlled by using different air flow rates as (a) 0, (b) 12, and (c) 24 L/min for the evaporation condition (dichloromethane evaporated at room temperature). The pores were found as (a) 0 μm, (b) 2.1 ± 1.2 μm, and (c) 3.0 ± 0.7 μm. (Right) Photographs of their yellow free-standing films.

formed with an air flow rate of 24 L/min. The images reveal regular pores (3.0 ± 0.7 μm) in the polymer. The SEM and EDS analyses showed the submicrorods to be KNdRu, which was randomly embedded within the pores of the polymer. Interestingly, when the air flow rate was decreased from 24 to 12 L/min in a separate experiment, the diameter of the pores decreased from 3.0 to 2.1 ± 1.2 μm [Figure 4b (left)], and around one-fifth of the polymer surface area was no longer covered by pores. A further decrease in the air flow rate to 0 L/min led to the pores' disappearance, giving the polymer a smooth surface [Figure 4a (left)].

Figure 5 summarizes the luminescent responses of the solid-supported KNdRu polymers to 200 ppm of putrescine at various exposure times. The polymer with the highest degree of porosity [Figure 5 (solid triangle)] exhibited the greatest enhancement in luminescence after exposure to the amine. Those with medium and low degrees of porosity [Figure 5 (solid square and circle, respectively)] underwent less obvious luminecence changes after such exposure (Supporting Information S. Figure 17). The insets of Figure 5 are photographs of the KNdRu polymer with a pore diameter of 3.0 μm, showing the naked-eye luminescent responses to putrescine at 0 and 120 min of exposure; its detection limit was found as 15 ppm.

Detection of Gaseous Biogenic Amines in Fish Sample by the Solid-Supported KNdRu Polymer. For final verification of the chemodosimetric idea, the solid-

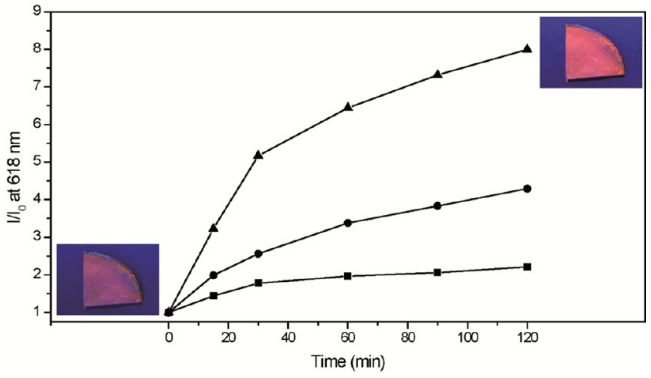

Figure 5. Luminescent responses of the solid supported KNdRu polymers toward 200 ppm of putrescine against time of exposure (solid triangle = the KNdRu polymer with pore diameter of 3.0 μm; solid circle = the KNdRu polymer with pore diameter of 2.1 μm; solid square = the KNdRu polymer with pore diameter of 0 μm). (Insets) The photographs of the naked-eyed luminometric responses of the solid supported KNdRu polymer (with pore diameter of 3.0 μm) after being subjected to putrescine for 120 min. Excitation λ_{ex} = 365 nm.

supported KNdRu polymer (pores diameter as 3.0 μm) was used to examine the real fish sample, Atlantic mackerel (*Scomber scombrus*). Figure 6 shows the spectrofluorimetric

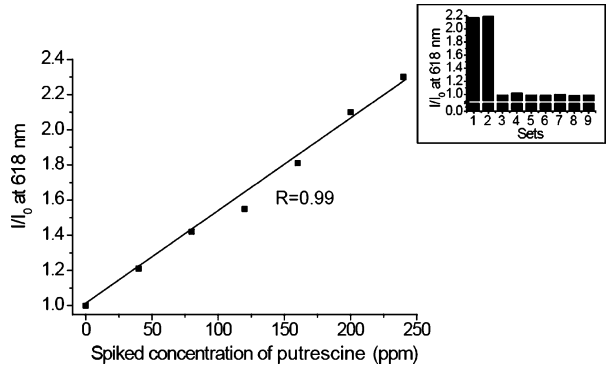

Figure 6. Spectrofluorimetric titration of the solid-supported KNdRu polymer (the polymer with pore diameter of 3.0 μm) toward 20.0 g of homogenized Atlantic mackerel spiked with increasing concentrations of putrescine (0 to 240 ppm). With the best fitted graph, I/I_0 versus [putrescine], the slope and y-intercept are 5.29 × 10^{-3} and 1, respectively. All titrations were carried out at 303 K. (Inset) Spectrofluorometric responses of the polymer toward the fish sample spiked with different analytes: (set 1) putrescine (200 ppm); (set 2) a mixture of putrescine and BVCs including aniline, H_2S, CO, CH_4, H_2, and N_2 (each of them is 200 ppm); (set 3–8) aniline, H_2S, CO, CH_4, H_2, and N_2 (200 ppm); and (set 9) a mixture of the BVCs used in sets 3–8 (each of them is 200 ppm).

responses of the polymer toward spiked putrescine (0 to 240 ppm) in the fish sample. Upon increasing the concentration of putrescine, a linear spectrofluorimetric response (R = 0.99) was obtained from the polymer. By plotting the best fitted graph, I/I_0 versus [spiked putrescine], the slope and y-intercept were calculated as 5.29 × 10^{-3} and 1, respectively. The spectrofluorimetric responses of the polymer toward a mixture of putrescine and BVCs showed similar results as that toward putrescine alone (inset of Figure 6, sets 1 and 2). However, there were no spectrofluorimetric changes of the polymer when spiking with either a mixture of BVCs or each of the vapors (Inset of Figure 6, sets 3–9). These results showed that other

dx.doi.org/10.1021/ac401513j | *Anal. Chem.* 2013, 85, 8246–8253

BVCs do not interfere with the luminescent responses of the polymer toward detection of putrescine.

CONCLUSION

Three new heterobimetallic Ru(II)−Ln(III) donor−acceptor complexes, KPrRu, KNdRu, and KSmRu, were synthesized and characterized in the study reported herein. Their photophysical and crystallographic data were also recorded. KPrRu, KNdRu, and KSmRu appear to be the first colorimetric and luminescent chemodosimeters selective for biogenic amine vapors with a detection limit as low as 10 ppb. The heterobimetallic chemodosimetric ensemble approach, in which one metal center acting as a function-specific binding site is bridged to another metal center responsible for signal transduction, seems to be a versatile way of designing new chemodosimeters and chemosensors. The submicrorods of these complexes, which feature a nanoscale diameter and microscale length, can be obtained through a simple precipitation process. Three yellow free-standing polymeric films with different degrees of porosity were fabricated by blending the submicrorods of the complexes with polystyrene polymer at various evaporation rates. The polymer with the highest level of porosity displayed the strongest luminescence enhancement after exposure to the amine.

ASSOCIATED CONTENT

Supporting Information

The synthetic procedures, the spectroscopic/spectrofluorimetric analyses, the crystallographic data of KPrRu, KNdRu, and KSmRu, and all of the UV−vis spectroscopic and spectrofluorometric titrations. This material is available free of charge via the Internet at http://pubs.acs.org.

AUTHOR INFORMATION

Corresponding Author

*E-mail: cfchow@ied.edu.hk.

Notes

The authors declare no competing financial interest.

ACKNOWLEDGMENTS

The work described in this paper was funded by a grant from the Hong Kong Institute of Education (Project Nos. R3321 and R3263) and a grant from the Research Grants Council of Hong Kong SAR, China (ECS No. 800312). Special thanks also go to Dr. Ho Yu Man and Mr. Chan Chun Ning of the City University of Hong Kong for their assistance with the SEM studies.

REFERENCES

(1) (a) Scallan, E.; Griffin, P. M.; Angulo, F. J.; Tauxe, R. V.; Hoekstra, R. M. *Emerging Infect. Dis.* **2011**, *17*, 16. (b) Scallan, E.; Hoekstra, R. M.; Angulo, F. J.; Tauxe, R. V.; Widdowson, M.-A.; Roy, S. L.; Jones, J. L. *Emerging Infect. Dis.* **2011**, *17*, 7.

(2) (a) Landete, J. M.; de las Rivas, B.; Marcobal, A.; Munoz, R. *Int. J. Food Microbiol.* **2007**, *117*, 258. (b) Bover-Cid, S.; Holzapfel, W. H. *Int. J. Food Microbiol.* **1999**, *53*, 33. (c) Lonvaud-Funel, A. *FEMS Microbiol. Lett.* **2001**, *199*, 9−13. (d) Halasz, A.; Barath, A.; Simonsarkadi, L.; Holzapfel, W. *Trends Food Sci. Technol.* **1994**, *5*, 42−49. (e) Stuart, A. E. *Neutron* **1999**, *22*, 431. (f) Jacobs, E. H.; Yamatodani, A.; Timmerman, H. *Trends Pharmacol. Sci.* **2000**, *21*, 293. (g) Taylor, S. L. *CRC Crit. Rev. Toxicol.* **1986**, *17*, 91. (h) Morrow, J. D.; Margolies, G. R.; Rowland, J.; Roberts, L. J. *N. Engl. J. Med.* **1999**, *324*, 716. (i) Bedry, R.; Gabinski, C.; Paty, M. *N. Engl. J. Med.* **2000**, *342*, 520. (j) *Decomposition & Histamine in Albacore, Skipjack, and Yellowfin Tuna*, FDA/ORA Compliance Policy Guide, 2004 revision, Subchapter 540.525; FDA: Washington, DC, 2004. (k) Bover-Cid, S.; Holzapfel, W. H. *Int. J. Food Microbiol.* **1999**, *53*, 33.

(3) (a) Chen, H. C.; Lee, Y. C.; Lin, C. M.; Hwang, D. F.; Tsai, Y. H. *Food Control* **2010**, *21*, 13. (b) Vinci, G.; Antonelli, M. L. *Food Control* **2002**, *13*, 519. (c) Calbiani, F.; Careri, M.; Elviri, L.; Mangia, A.; Pistara, L.; Zagnoni, I. *J. Agric. Food Chem.* **2005**, *53*, 3779. (d) Landete, J. M.; Ferrer, S.; Polo, L.; Pardo, I. *J. Agric. Food Chem.* **2005**, *53*, 1119. (e) Paleologos, E. K.; Kontominas, M. G. *Anal. Chem.* **2004**, *76*, 1289. (f) Duflos, G.; Dervin, C.; Malle, P.; Bouquelet, S. *J. AOAC Int.* **1999**, *82*, 1097.

(4) (a) Onal, A. *Food Chem.* **2007**, *103*, 1475. (b) Chiu, T. C.; Lin, Y.-W.; Huang, Y.-F.; Chang, H.-T. *Electrophoresis* **2006**, *27*, 4792. (c) Bao, L.; Sun, D.; Tachikawa, H.; Davidson, V. L. *Anal. Chem.* **2002**, *74*, 1144. (d) Oguri, S.; Okuya, Y.; Yanase, Y.; Suzuki, S. *J. Chromatogr., A* **2008**, *1202*, 96. (e) Paleologos, E. K.; Kontaminas, M. G. *Anal. Chem.* **2004**, *76*, 1289. (f) Oguri, S.; Yoneya, Y.; Mizunuma, M.; Fujiki, Y.; Otsuka, K.; Terabe, S. *Anal. Chem.* **2002**, *74*, 3463. (g) Ruiz-Capillas, C.; Moral, A. *J. Food. Sci.* **2001**, *66*, 1030. (h) Rossi, S.; Lee, C.; Ellis, P. C.; Pivarnlik, L. F. *J. Food. Sci.* **2002**, *67*, 2056. (i) Sun, X.; Yang, X.; Wang, E. *J. Chromatog., A* **2003**, *1005*, 189.

(5) (a) Greene, N. T.; Shimizu, K. D. *J. Am. Chem. Soc.* **2005**, *15*, 5695. (b) Mertz, E.; Zimmerman, S. C. *J. Am. Chem. Soc.* **2003**, *125*, 3424−3425. (c) Yeh, C.; Lin, S.; Hwang, D. *J. Food Drug Anal.* **2004**, *12*, 128−132. (d) Kubota, S.; Okada, M.; Imahori, K.; Ohsawa, N. *Cancer Res.* **1983**, *43*, 2363−2367. (e) Xu, C. X.; Marzoul, S. A. M.; Cosafret, V. V.; Buck, R. P.; Neuman, M. R.; Sprinkle, R. H. *Talanta* **1997**, *44*, 1625−1632. (f) Luong, J. H. T.; Hrapovic, S.; Wang, D. *Electroanalysis* **2005**, *17*, 47−53.

(6) (a) Korsten, S.; Mohr, G. J. *Chem.−Eur. J.* **2011**, *17*, 969. (b) Reinert, S.; Mohr, G. J. *Chem. Commun.* **2008**, *47*, 2272. (c) Mohr, G. J. *Chem.−Eur. J.* **2004**, 1082−1090. Mohr, G. J. *Anal. Chim. Acta* **2004**, *508*, 233−237. (d) Mohr, G. J. *Dyes Pigm.* **2004**, *62*, 77−81. (e) Mohr, G. J.; Klimant, I.; Spichiger-Keller, U. E.; Wolfbeis, O. S. *Anal. Chem.* **2001**, *74*, 1053−1056. (f) Lee, B.; Scopelliti, R.; Severin, K. *Chem. Commun.* **2011**, *47*, 9639−9641. (g) Patze, C.; Broedner, K.; Rominger, F.; Trapp, O.; Bunz, U. H. F. *Chem.−Eur. J.* **2011**, *17*, 13720−13725. (h) Kostereli, Z.; Severin, K. *Chem. Commun.* **2012**, *48*, 5841−5843. (i) Jung, J. H.; Lee, S. J.; Kim, J. S.; Lee, W. S.; Sakata, Y.; Kaneda, T. *Org. Lett.* **2006**, *8*, 3009−3012. (j) Secor, K.; Plante, J.; Avetta, C.; Glass, T. *J. Mater. Chem.* **2005**, *15*, 4073−4077. (k) Jung, J. H.; Lee, H. Y.; Jung, S. H.; Lee, S. J.; Sakata, Y.; Kaneda, T. *Tetrahedron* **2008**, *64*, 6705−6710.

(7) (a) Chow, C. F.; Kong, H. K.; Leung, S. W.; Chiu, B. K. W.; Koo, C. K.; Lei, E. N. Y.; Lam, M. H. W.; Wong, W. T.; Wong, W. Y. *Anal. Chem.* **2011**, *83*, 289−296. (b) Guo, Q.-N.; Li, Z.-Y.; Chan, W.-H.; Lau, K.-C.; Crossley, M. J. *Supramol. Chem.* **2010**, *22*, 122. (c) Seto, D.; Soh, N.; Nakano, K.; Imato, T. *Anal. Biochem.* **2010**, *404*, 135. (d) Seto, D.; Soh, N.; Nakano, K.; Imato, T. *Bioorg. Med. Chem. Lett.* **2010**, *20*, 6708.

(8) Ikeda, M.; Yoshii, T.; Matsui, T.; Tanida, T.; Komatsu, H.; Hamachi, I. *J. Am. Chem. Soc.* **2011**, *133*, 1670.

(9) (a) Maynor, M. S.; Nelson, T. L.; O'Sullivan, C.; Lavigne, J. J. *Org. Lett.* **2007**, *9*, 3217−3220. (b) Nelson, T. L.; Tran, I.; Ingallinera, T. G.; Maynor, M. S.; Lavigne, J. J. *Analyst* **2007**, *132*, 1024−1030. (c) Nelson, T. L.; O'Sullivan, C.; Greene, N. T.; Maynor, M. S. *J. Am. Chem. Soc.* **2006**, *128*, 5640. (d) English, J. T.; Deore, B. A.; Freund, M. S. *Sens. Actuators, B: Chem.* **2006**, *115*, 666−671.

(10) (a) Kim, T. I.; Park, J.; Kim, Y. *Chem.−Eur. J.* **2011**, *17*, 11978. (b) Che, Y.; Zang, L. *Chem. Commun.* **2009**, 5106−5108. (c) Qiu, L. G.; Li, Z. Q.; Wu, Y.; Wang, W.; Xu, T.; Jiang, X. *Chem. Commun.* **2008**, 3642−3644.

(11) (a) Mader Heike, S.; Wolfbeis, O. S. *Anal. Chem.* **2010**, *82*, 5002. (b) Azab, H. A.; EI-Korashy, S. A.; Anwar, Z. M.; Khairy, G. M.; Steiner, M.-S.; Duerkop, A. *Analyst* **2011**, *136*, 4492. (c) Steiner, M. S.; Meier, R. J.; Duerkop, A.; Wolfbeis, O. S. *Anal. Chem.* **2010**, *82*, 8402−8405.

(12) (a) Cho, D.-G.; Sessler, J. L. *Chem. Soc. Rev.* **2009**, *38*, 1647. (b) Du, J.; Hu, M.; Fan, J.; Peng, X. *Chem. Soc. Rev.* **2012**, *41*, 4511.
(13) (a) Chae, M. Y.; Czarnik, A. W. *J. Am. Chem. Soc.* **1992**, *114*, 9704. (b) Czarnik, A. W.; Dujols, V.; Ford, F. *J. Am. Chem. Soc.* **1997**, *119*, 7386.
(14) (a) Moragues, M. E.; Martinez-Manez, R.; Sancenon, F. *Chem. Soc. Rev.* **2011**, *40*, 2593. (b) Nguyen, B. T.; Anslyn, E. V. *Coord. Chem. Rev.* **2006**, *250*, 3118.
(15) (a) Lavigne, J. L.; Anslyn, E. V. *Angew. Chem., Int. Ed.* **1999**, *38*, 3666. (b) Wiskur, S. L.; Anslyn, E. V. *J. Am. Chem. Soc.* **2001**, *123*, 10109. (c) Alt-Haddou, H.; Wiskur, S. L.; Lynch, V. M.; Anslyn, E. V. *J. Am. Chem. Soc.* **2001**, *123*, 11296. (d) Schneider, S. E.; O'Neil, S. N.; Anslyn, E. V. *J. Am. Chem. Soc.* **2000**, *122*, 542. (e) Zhong, Z.; Anslyn, E. V. *J. Am. Chem. Soc.* **2002**, *124*, 9014.
(16) (a) Fabbrizzi, L.; Leone, A.; Taglietti, A. *Angew. Chem., Int. Ed.* **2001**, *40*, 3066. (b) Fabbrizzi, L.; Foti, F.; Taglietti, A. *Org. Lett.* **2005**, *7*, 2603. (c) Hortala, M. A.; Fabbrizzi, L.; Marcotte, N.; Stomeo, F.; Taglietti, A. *J. Am. Chem. Soc.* **2003**, *125*, 20. (d) Amendola, V.; Bergamaschi, G.; Buttafava, A.; Fabbrizzi, L.; Monzani, E. *J. Am. Chem. Soc.* **2010**, *132*, 147.
(17) (a) Jimenez, D.; Martinez-Manez, R.; Sancenon, F.; Ros-Lis, J. V.; Benito, A.; Soto, J. *J. Am. Chem. Soc.* **2003**, *125*, 9000. (b) Comes, M.; Rodriguez-Lopez, G.; Marcos, M. D.; Martinez-Manez, R.; Sancenon, F.; Soto, J.; Villaescusa, L. A.; Amoros, P.; Beltran, D. *Angew. Chem., Int. Ed.* **2005**, *44*, 2918. (c) Martinez-Manez, R.; Sancenon, F. *Chem. Rev.* **2003**, *103*, 4419. (d) Martinez-Manez, R.; Sancenon, F.; Biyikal, M.; Hecht, M.; Rurack, K. *J. Mater. Chem.* **2011**, *21*, 12588.
(18) (a) Chow, C. F.; Chiu, B. K. W.; Lam, M. H. W.; Wong, W. Y. *J. Am. Chem. Soc.* **2003**, *125*, 7802. (b) Chow, C. F.; Lam, M. H. W.; Wong, W. Y. *Dalton Trans.* **2005**, *3*, 475. (c) Chow, C. F.; Lam, M. H. W.; Wong, W. Y. *Inorg. Chem.* **2004**, *43*, 8387. (d) Koo, C. K.; Chow, C. F.; Chiu, B .K. W.; Lam, M. H. W.; Wong, W. Y. *Eur. J. Inorg. Chem.* **2008**, 1318. (e) Chow, C. F.; Kong, H. K.; Leung, S. W.; Chiu, B. K. W.; Koo, C. K.; Lei, E. N. Y.; Lam, M. H. W.; Wong, W. T.; Wong, W. Y. *Anal. Chem.* **2011**, *83*, 289.
(19) (a) Palomares, E.; Vilar, R.; Green, A.; Durrant, J. R. *Adv. Funct. Mater.* **2004**, *14*, 111. (b) Obare, S. O.; Hollowell, R. E.; Murphy, C. J. *Langmuir* **2002**, *18*, 10407. (c) Mercier, L.; Pinnavaia, T. J. *Adv. Mater.* **1997**, *9*, 500. (d) Boiocchi, M.; Fabbrizzi, L.; et al. *Angew. Chem., Int. Ed.* **2004**, *43*, 3847.
(20) (a) Ward, M. D. *Coord. Chem. Rev.* **2006**, *250*, 3128−3141. (b) Herrera, J.-M.; Pope, S. J. A.; Adams, H.; Faulkner, S.; Ward, M. D. *Inorg. Chem.* **2006**, *45*, 3895−3904. (c) Baca, S. G.; Pope, S. J. A.; Adams, H.; Ward, M. D. *Inorg. Chem.* **2008**, *47*, 3736−3747. (d) Davies, G. M.; Pope, S. J. A.; Adams, H.; Faulkner, S.; Ward, M. D. *Inorg. Chem.* **2005**, *44*, 4656−4665. (e) Miller, T. A.; Jeffery, J. C.; Ward, M. D.; Adams, H.; Pope, S. J. A.; Faulkner, S. *Dalton Trans.* **2004**, 1524−1526. (f) Chen, Y. J.; Xie, P. H.; Endicott, J. F. *J. Phys. Chem. A* **2004**, *108*, 5051−5049. (g) Chen, Y. J.; Odongo, O. S.; McNamara, P. G.; Szacilowski, K. T.; Endicott, J. F. *Inorg. Chem.* **2008**, *47*, 10921−10937. (h) Bernhardt, P. V.; Bozoglian, F.; Macpherson, B. P.; Martinez, M. *Coord. Chem. Rev.* **2005**, *249*, 1902−1916. (i) Li, D. F.; Clerac, R.; Roubeau, O.; Harte, E.; Mathoniere, C.; Le Bris, R.; Holmes, S. M. *J. Am. Chem. Soc.* **2008**, *130*, 252−258.
(21) Synthetic procedures and spectroscopic/spectrofluorimetric analyses are described in detail in the Supporting Information.
(22) (a) Demas, J. N.; Turner, T. F.; Crosby, G. A. *Inorg. Chem.* **1969**, *8*, 674. (b) Krause, R. A. *Inorg. Chim. Acta* **1977**, *22*, 209. (c) Kato, M.; Yamauchi, S.; Hirota, N. *J. Phys. Chem.* **1989**, *93*, 3422.
(23) (a) Peterson, S. H.; Demas, J. N. *J. Am. Chem. Soc.* **1976**, *98*, 7880. (b) Peterson, S. H.; Demas, J. N. *J. Am. Chem. Soc.* **1979**, *101*, 6571.
(24) Bignozzi, C. A.; Chiorboli, C.; Indelli, M. T.; Rampi-Scandola, M. A.; Varani, G.; Scandola, F. *J. Am. Chem. Soc.* **1986**, *108*, 210.
(25) Shriver, D. F.; Posner, J. *J. Am. Chem. Soc.* **1966**, *88*, 1672.
(26) (a) Campagna, S.; Serroni, S. *Chem. Rev.* **1996**, *96*, 759. (b) Bartocci, C.; Bignozzi, C. A.; Scandola, F.; Rumin, R.; Courtot, P. *Inorg. Chim. Acta* **1983**, *76*, L119. (c) Bignozzi, C. A.; Scandola, F. *Inorg. Chem.* **1984**, *23*, 1540.
(27) Connors, K. A. *Binding Constants, The Measurement of Molecular Complexes Stability*; John Wiley and Sons: New York, 1987.
(28) (a) Bernards, D. A.; Desai, T. A. *Soft Matter* **2010**, *6*, 1621. (b) Madou, M. J. *Fundamentals of Microfabrication*, 2nd ed.; CRC Press: Boca Raton, FL, 2002. (c) Metters, A. T.; Anseth, K. S.; Bowman, C. N. *Polymer* **2000**, *41*, 3993. (d) Walker, J. C.; Kendal-Reed, M.; Hall, S. B.; Morgan, W. T.; Polyakov, V. V.; Lutz, R. W. *Chem. Senses* **2001**, *26*, 351.
(29) (a) Ulbricht, M. *Polymer* **2006**, *47*, 2217. (b) Pall Corporation. *Polysulfone Membranes*; Pall Corporation: Port Washington, NY, 2009. (c) Whatman. *Polysulfone Membranes*; Whatman: Piscataway, NJ, 2009.